Dalton Transactions

PAPER

Isolation of EPR spectra and estimation of spin-states in two-component mixtures of paramagnets

Sonia Chabbra,[a] David M. Smith [b] and Bela E. Bode *[a]

Received 00th January 20xx,
Accepted 00th January 20xx

DOI: 10.1039/x0xx00000x

www.rsc.org/

The presence of multiple paramagnetic species can lead to overlapping electron paramagnetic resonance (EPR) signals. This complication can be a critical obstacle for the use of EPR to unravel mechanisms and aid the understanding of earth abundant metal catalysis. Furthermore, redox or spin-crossover processes can result in the simultaneous presence of metal centres in different oxidation or spin states. In this contribution, pulse EPR experiments on model systems containing discrete mixtures of Cr(I) and Cr(III) or Cu(II) and Mn(II) complexes demonstrate the feasibility of the separation of the EPR spectra of these species by inversion recovery filters and the identification of the relevant spin states by transient nutation experiments. We demonstrate the isolation of component spectra and identification of spin states in a mixture of catalyst precursors. The usefulness of the approach is emphasised by monitoring the fate of the chromium species upon activation of an industrially used precatalyst system.

Introduction

Over 80% of compounds produced by the chemical industries encounter one or more catalytic transformation during their making. As a result of global market expansion catalysis continues to be an area of academic and industrial research. Aspects of major importance are the cost reduction possible by replacing precious metals with earth-abundant ones.[1] Furthermore, increasing sustainability and avoiding waste products is becoming a major driver in the field.[2] Mechanisms of homogeneous catalysis are often successfully investigated by nuclear magnetic resonance (NMR) spectroscopy.[3, 4] However, many transition metal catalysts undergo redox changes during their reactions giving rise to paramagnetic intermediates and leading to broadened NMR spectra that hamper analysis. Electron paramagnetic resonance (EPR) spectroscopy is exclusively and exquisitely sensitive to the unpaired electrons of paramagnetic centres making it an excellent tool to examine their electronic and geometric structures.[5, 6] The exclusive sensitivity to paramagnets has the advantage that even high concentrations of different diamagnetic species will not obscure the signal of the paramagnet. Especially interactions with magnetic nuclei can be highly informative as the strength of the interaction between the electron spins and the nuclear spins will reveal insights into the electronic orbitals harbouring the electron spins and their distance to the nuclei in question. One example involving different paramagnetic oxidation states is chromium-based ethylene oligomerisation catalysis.[7, 8] A wide range of chromium complexes containing bidentate and tridentate ligands have been developed for the selective oligomerisation. The formation of linear α-olefins (such as 1-butene, 1-hexene, 1-octene etc.) is achieved by using an active catalyst under ethylene pressure. This catalyst is formed by adding an activator such as methylaluminoxane (MAO), modified methylaluminoxane (MMAO), a combination of triethylaluminium (Et_3Al) and a weakly coordinating anion such as $[B(C_6F_5)_4]^-$ or $[Al(OC(CF_3)_3)_4]^-$ to a solution of chromium precursor complex and a PNP (PNP = $Ph_2PN(R)PPh_2$) ligand. In general, the activator behaves as a co-catalyst, it can replace the anion in some cases and acts as alkylating and reducing agent thereby transforming Cr(III) precursors to Cr(I).[9] The product distribution and catalyst viability are highly dependent on the exact choice of precatalyst composition and equivalents of the activator employed. By far the most efficient catalyst facilitating ethylene tetramerisation comprises of the highly active Cr/PNP system with MMAO as an activator. This system shows up to 70% selectivity for 1-octene over side-products including other linear α-olefins.[10] Additionally, the solvent plays a crucial role for activity and selectivity. As demonstrated by EPR, in toluene the catalyst system forms a PNP-free Cr(I) sandwich complex $[Cr(\eta^6\text{-}CH_3C_6H_5)_2]^+$ which is inactive for olefin oligomerisation.[11] However, some aromatic solvents facilitate olefin oligomerisation with good activities.[9] Substantial efforts have been made to improve catalyst efficiency and to unravel the underlying mechanisms.[7, 8] However, the presence of species with different electron spin states and their overlapping spectra complicate EPR analysis. Hence, in this article we explore pulse EPR experiments on a model system containing a mixture of discrete Cr(I)[12, 13] and Cr(III)[7] complexes used as catalyst precursors in ethylene tetramerisation catalysis. The separation

[a] EaStCHEM School of Chemistry and Centre of Magnetic Resonance, University of St Andrews, St Andrews, Fife, KY16 9ST, Scotland, U.K.
*E-mail: beb2@st-andrews.ac.uk
[b] Sasol UK Ltd, St Andrews, Fife, KY16 9ST, Scotland, U.K.

†Electronic Supplementary Information (ESI) available: Analytical data and additional samples and their EPR data. See DOI: 10.1039/x0xx00000x. The research data supporting this publication can be accessed at DOI: 10.17630/255feac7-f9e5-4690-a351-87be9842b266

of the overlapping spectra and the estimation of spin states were tested by using an inversion recovery filter[14, 15] (IRf) combined with echo detected field sweep and transient nutation[16] experiments. IRf field sweep experiments have been tested previously on a mixture comprising TEMPO (2,2,6,6-tetra-methyl-piperidine-1-oxyl) and BDPA (α,γ-bisphenylene-β-phenylallyl-benzolate) organic radicals in polystyrene to isolate their individual spectra.[15] This method has allowed isolating the overlapping EPR signals of the iron-sulphur clusters N1 and N2 in mitochondrial complex 1 as demonstration for electron spin (*S*) 1/2 systems.[15] Here, we seek to expand this method to mixtures containing $[Cr(I)(CO)_4(({}^{i}Pr)PNP)][Al(OC(CF_3)_3)_4]$ (**1**) and tris(2,2,6,6-tetramethyl-3,5-heptanedionato)chromium(III) (**2**) as *S* = 1/2 and *S* = 3/2 systems. The different total electron spin will in turn alter the transition dipole moment and thus the nutation frequency. Transient nutation experiments have been exemplified on MgO single crystals[17] doped with different transition metal ions such as Mn^{2+}, V^{2+} and Cr^{3+} as well as a photo-excited triplet state of pentacene crystals.[18] The experiments enable identification of electron spin quantum number and assign corresponding electron-spin transitions. Furthermore, PEANUT (Phase-inverted echo-amplitude detected nutation) experiments on γ-irradiated Herasil quartz and Mn^{2+} doped $CaCO_3$ powder[19] or single crystals of an ionic anthracene aggregate with triplet ground state[20] have allowed separating EPR spectra by electron spin state. Herein we are probing catalytically relevant intermediates with broad EPR lines and fast relaxation times, which make advanced experiments challenging. Thus, in this contribution we focus on the use of the most experimentally robust transient nutation experiments. The general applicability of these pulse EPR experiments is shown on a model system comprising a mixture of well-studied terpyridine complexes of Cu(II)[21, 22] (**3**) and Mn(II)[23] (**4**). This approach is validated on another model system of Cr(I) and Cr(III) catalyst precursors relevant to ethylene oligomerisation and further extended to a solution of activated precatalyst mixture. This constitutes the first application of these pulse EPR approaches to chromium species relevant to catalytic ethylene oligomerisation.

Results and Discussion

The pulse sequence used for the inversion recovery filtered (IRf) field sweep experiment is shown in the Figure 1(a). In the conventional inversion recovery experiment, the π pulse flip the spins thereby inverting the ensemble magnetisation (to $-M_z$), and then during the time T the electron spins relax back towards the equilibrium magnetisation, M_z, with their longitudinal relaxation time constant (T_1). The resulting longitudinal magnetisation is read out by a Hahn echo detection sequence ($\pi/2-\tau-\pi-\tau$) applied at different times T. T_1 can be measured by recording the Hahn echo intensity as a function of T. If the two species in a binary mixture differ by orders of magnitude in T_1, this pulse sequence can potentially be used to filter individual spectra from the mixture. Setting T to a constant filter time (T_F), where magnetisation of one species is exactly zero will suppress this species' contribution to the echo. Sweeping the magnetic

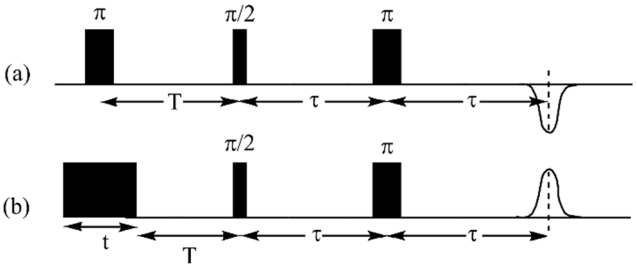

Figure 1 The pulse sequences for (a) Inversion Recovery and (b) echo detected transient nutation.

field now isolates the spectrum of the other species having nonzero magnetisation at the given time T. Performed at the two corresponding filter times, this experiment potentially allows to recover the individual spectra from a binary mixture. The underpinning assumption is that the entire spectrum of this species displays a single inversion recovery rate independent of orientation or transition.

For a mixture containing two discrete complexes, the echo can be optimised by adjusting the amplitude and length of the detection pulses. The angle of rotation (β) of the z-magnetisation by an on-resonance microwave pulse often called flip-angle is given in eq. 1:

$$\beta = \omega_{nut} t_p \quad (1)$$

where, t_p is the pulse length and ω_{nut} is nutation frequency which depends on total spin (*S*) of the system. For the transition between the m_s and m_s+1 magnetic sublevels ω_{nut} is given by eq. 2:

$$\omega_{nut}(m_S, m_S+1) = \omega_1\sqrt{S(S+1) - m_s(m_s+1)} \quad (2)$$

For a spin *S* = 1/2 species the nutation frequency is equal to the microwave field strength in angular frequency units ω_1 that is given by $\omega_1 = g_{eff}\mu_\beta B_1/\hbar$ where g_{eff} is effective *g* factor, μ_B is Bohr magneton, B_1 is microwave field strength (in frequency units) and $\hbar$ is as the reduced Plank constant.

To demonstrate the effects of different pulse parameters we chose a model mixture of terpyridine complexes of Cu(II)(**3**) and

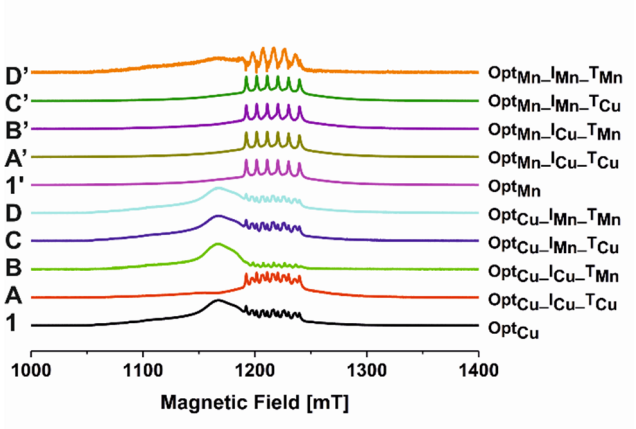

Figure 2 Echo detected field sweep experiments were performed at Q-band (~34 GHz) for both species in a mixture of **3** and **4** using optimum parameters for their detection (D_{Cu} or D_{Mn}), suppression (filter times T_F^{Cu} or T_F^{Mn}) and inversion (I_{Cu} or I_{Mn}). The length of the inversion pulse was set to 20 ns for I_{Cu} and 12 ns for I_{Mn} in combination with a T_F^{Cu} of 214 μs and T_F^{Mn} of 18 μs to recover the spectra of **4** and **3** from spectrum 1 (A to D) and 1' (A' to D').

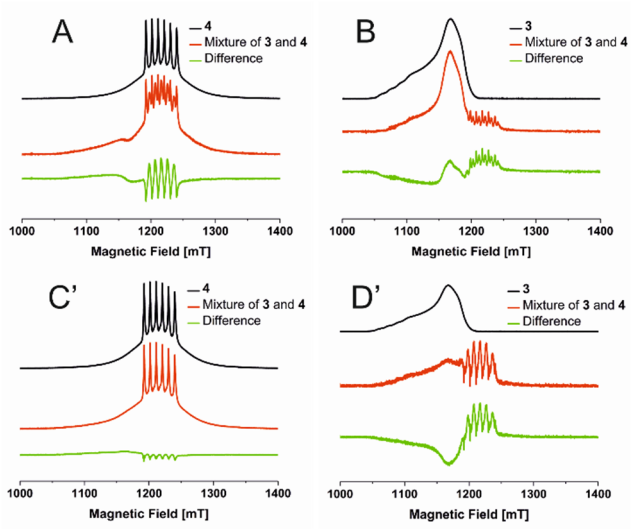

Figure 3 Comparison of pure samples of **3** and **4** with the spectra obtained from their mixture at different conditions (as shown in Figure 2). Panels A and B show the spectra of **4** and **3** recovered from the mixture while optimising the echo forming and inversion pulses in the Cu(II) spectrum with T_Fs equal to 18 μs and 214 μs, respectively. The same T_Fs were used in combination with optimising the echo forming and inversion pulses in the Mn(II) spectrum (Panel C' and D').

Mn(II)(**4**). These complexes are well known to have S = 1/2 and S = 5/2 ground states and the nutation frequency of their $m_s = -1/2$ to $m_s = +1/2$ transition should scale by a factor of 3. For complexes with different spin states, ω_{nut} will differ even at identical ω_1 and this will have to be compensated to achieve identical flip angles β. Thus, either t_P, ω_1 or both will have to be adjusted (eq. 1). Therefore, strictly only one transition of one spin state can be optimally inverted and refocussed to form an echo by the detection sequence (Figure 2, spectra 1 and 1'). Furthermore, the optimal length and microwave field strength of the inversion pulse will again be different for species with different total electron spin. This increases the number of parameters (in addition to T_F) needed in order to isolate individual spectra from a mixture as described above. As a result, either species (copper or manganese) display optimum parameters for their detection (D_{Cu} or D_{Mn}), suppression (filter times T_F^{Cu} or T_F^{Mn}) and inversion (I_{Cu} or I_{Mn}). This leads to eight possible combinations of experimental settings for performing the IRf field sweep experiment as shown in Figure 2. The inversion recovery experiments for **3** and **4** were performed at the positions with maximum signal. However, for high spin systems such as Mn(II) in **4** having S = 5/2, transitions other than $m_s = -1/2$ to $m_s = +1/2$ can take place. These additional transitions have different nutation frequencies and might also display altered relaxation times. As a result, it is difficult to isolate the pure spectrum of **3** from the mixture. The spectrum of **3** most closely resembling pure **3** was retrieved by optimising the echo forming and inversion pulses in the spectrum of **3** while using a T_F of 18 μs (corresponding to a zero-crossing in the inversion recovery experiment on pure **4**). Nevertheless, there is still a significant contribution of **4** to the filtered spectrum (Figure 3, Panel B). On the other hand, optimising the amplitude of the echo forming pulses in the spectrum of **4** diminished the

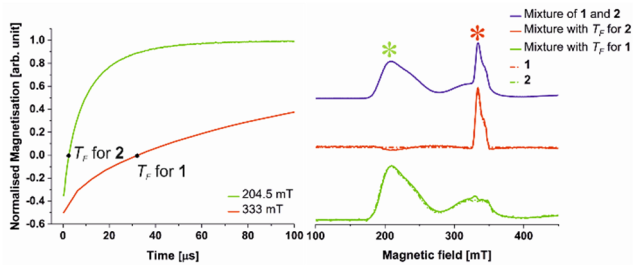

Figure 4 The inversion recovery traces recorded for both species in the mixture of **1** and **2** at X-band (9 GHz) at 12 K by using the pulse sequence shown in Figure 1(a) are shown on the left. Inversion recovery filtered field sweep spectra are displayed on the right and use the same pulse sequence with constant filter times of 2.6 μs and 32 μs to recover the respective spectra of **1** and **2** from the mixture.

contribution of **3** to all spectra, which renders the isolation more challenging (Figure 3, Panel D'). Similarly, the spectrum for **4** can be recovered by optimizing the echo forming and inversion pulses in the spectrum of **4** while using a T_F of 214 μs (Figure 3, Panel C') the zero-crossing in the inversion recovery experiment on pure **3**. For a quantitative comparison of the recovered spectra with pure components, they were scaled to minimise the root mean square deviation between the recovered and pure spectra shown in Figure 3.

This experiment was then validated on the second system containing a mixture of low spin Cr(I) in **1** and the S = 3/2 Cr(III) in **2**. Both metal precursors are relevant to Cr/PNP based ethylene tetramerisation catalysis and their spectroscopic data are shown in Figure 4 (right, blue). The longitudinal relaxation time constants, T_1 were obtained from inversion recovery experiments at the field positions shown with asterisk symbols. The raw data was phase corrected and fitted using a biexponential. Commonly, the faster time constant in inversion recovery experiments is attributed to the spectral diffusion rate. This rate describes exchange of magnetisation between the inverted spins and those spectrally close spins not inverted due to the finite microwave excitation bandwidth.[16] The slower time constant is most often dominated by T_1 relaxation. At 12 K, T_1 was determined to 200 μs and 16 μs for **1** and **2**, respectively. Due to the convoluted effects of spectral diffusion and T_1 relaxation, the filter times were directly chosen as the experimental zero crossings of the inversion recovery experiments. The IRf field sweep was recorded by optimising the inversion pulse in a spectral region belonging to **1** and using a T_F of 32 μs to obtain a filtered spectrum of **2** as shown in Figure 4 (right, green). The same procedure optimising the inversion pulse in a region belonging to the spectrum of **2** and using a T_F of 2.6 μs was repeated to recover the spectrum of **1** (Figure 4 right, red).

It has been shown that IRf echo detected field sweep experiments work well for both model systems and can be used to isolate overlapping spectra of a binary mixture. In literature, this concept had already been tested on mixtures containing S = 1/2 radicals such as BDPA and TEMPO and applied on iron-sulphur clusters in proteins.[15] The methodology had further been extended to two-dimensional Inversion Recovery experiments for the extraction of more than two components.[24]

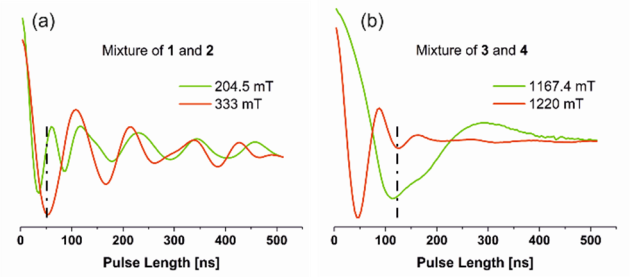

Figure 5 The time domain data obtained from transient nutation experiment at 10 K are shown for the mixture of **1** and **2** (left) and **3** and **4** (right) measured at X- and Q-band, respectively. A vertical dashed line in black shows the point of comparison in the corresponding traces. The frequency ratio agrees with predictions from eq. 2.

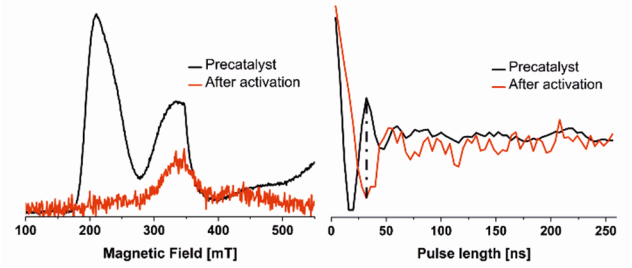

Figure 6 The precatalyst comprising a mixture of Cr(III) precursor **2**, ligand ^{i}PrPNP and anion L-CAB in 4-Cl-tol. The precatalyst was activated by addition of 10 equivalents of Et_3Al and measured after 1.5 hrs. The echo detected field sweep experiment performed at 10 K is shown on the left. The time domain data obtained from transient nutation experiments are shown on the right and the point of comparison is shown by a vertical dashed line in black.

However, here the focus is application to systems containing different electron spin states. Complexes with $S > 1/2$ often result into broad spectra and complicate analysis due to contributions from different allowed transitions. In addition, the spins in these complexes often relax very fast leading to very small signals. This can be confounded with different relaxation times for different transitions. Here, we have limited the experiments to one dimension as this is sufficient to filter the spectra of a binary mixture. In conclusion, the best way to recover individual spectra of any species from a mixture is by optimising the echo forming pulses in the spectrum of the species to be extracted. If the contribution of other species is minimal (such as **3** when optimising the Hahn echo on **4**), then this might already be sufficient for separation. In general, optimising the inversion pulse in the spectrum to be isolated and setting T_F to the zero crossing of the spins belonging to the other spectrum will help extracting one species. Optimisation positions and filter times can simply be interchanged to the respective other species to extract the other spectrum. In an unknown spectrum where the single contributions cannot readily be allocated to different species it seems most sensible to optimise inversion and detection pulses in different parts of the spectrum and record with both filter times. However, inhomogeneous broadening often leads a distribution in nutation frequencies leading to small differences between the inversion and detection parameters. This was observed in the mixture of Cr(I) (**1**) and Cr(III) (**2**). In this case, both species can be satisfactorily recovered from the same inversion and detection parameters using the corresponding T_F. In conclusion, IRf echo detected field sweep experiments allow the isolation of overlapping spectra of binary mixtures. Importantly, for mixtures containing three or more species with different relaxation times, only a single one can be supressed. It is important to note that transverse relaxation can also be field-dependent and nuclear modulation frequencies do depend on field. This means the appearance of field swept EPR spectra can become complicated to interpret especially for very anisotropic systems and in presence of strong nuclear modulation.

In order to gain further insight into the species formed after activation and potentially assign their oxidation states *via* the electron spin state, transient nutation experiments can be performed. The possible electron spin states are limited by the oxidation state and ligand field of a transition metal. *Vice versa* the observation of certain spin states limits the possible oxidation states. Thus, nutation measurements can help understanding paramagnetic intermediates. To this end, we explored this opportunity at field positions corresponding to the different pure species in the mixtures of **1** and **2** and of **3** and **4**. The pulse sequence used is shown in Figure 1 (b) where the length of the first pulse is incremented and the resulting rotation of the initial magnetisation is measured by a Hahn echo detection sequence ($\pi/2–\tau–\pi–\tau$) in order to record a nutation profile as a function of pulse length. The lengths of the optimum inversion pulses depend on spin state and the magnetic sublevels involved in the transition (eq. 2). The time domain data obtained from transient nutation experiments is shown in Figure 5 for both mixtures. In Figure 5 (a), the electron spin of **2** initially nutates (shown in green) by a factor of two faster than the electron spin in **1** (nutation shown in red) which is in accordance with the ratio of frequencies (ω_{nut}) calculated for $S = 1/2$ and $S = 3/2$ for a transition between the $m_s = -1/2$ and $m_s+1 = +1/2$ levels (eq. 2). The minimum in the first oscillation in the nutation curve of **1** coincides with the maximum after the first period of oscillation in the nutation profile of **2**, corresponding to a factor of two in initial frequency. Using longer nutation pulse lengths leads to a dephasing of oscillations which we tentatively attribute to inhomogeneous line widths and the distribution of excitation strength in the EPR probehead. It is well established, that broad EPR lines, the occurrence of multiple (allowed and forbidden) electron spin transitions and admixture of nuclear spin lead to additional frequency contributions and broadenings that complicate the situation significantly.[16] Nevertheless, the comparison of initial frequencies is reliable for a range of known samples as demonstrated in the supporting information. This has also been demonstrated on the mixture of **3** and **4** as shown in Figure 5(b). The nutation frequency calculated for a transition between $m_s = -1/2$ and $m_s+1 = +1/2$ of $S = 5/2$ is three times faster than for $S = 1/2$. The time of the first minimum in **3** (*i.e.* half a modulation) coincides with the second minimum of **4** (*i.e.* one and a half modulations) corresponding to a frequency ratio of three (Figure 5(b)) as calculated above. Hence, nutation experiments can help understanding an intermediate species formed after catalyst activation by assigning a spin state to

individual peaks. However, this will become more involved if there are significant contributions from two or more spin states. As described above, activation of precatalyst results in various species with different oxidation states. To demonstrate the scope of the methodology, the insights gained on the model systems were transferred to the activated catalyst mixture. The precatalyst comprising a mixture of **2**, ^{i}PrPNP ligand and an ammonium borate salt in 4-Cl-tol. This precatalyst was activated by addition of 10 equivalents of Et_3Al at room temperature and the sample was frozen after 1.5 hrs before recording an echo detected field sweep spectrum at 10 K. The majority of the EPR signal is lost after activation. The activation of Cr(III) catalyst precursors is known to lead to reduction to Cr(I) and further speciation into different EPR silent oxidation states and/or dimers has been studied.[11] The remaining small EPR signal led to reduced signal-to-noise in pulse EPR experiments despite increased averaging time. The transient nutation profiles of these samples are shown in Figure 6. The full oscillation of the precatalyst coincides with first half modulation (*i.e.* minimum) the species formed after activation. From eq. 2, this confirms that the new species nutates with frequency of $S = 1/2$. Thus, this data fully confirms the conclusion that Cr(III) present in the precatalyst is reduced to form Cr(I) after activation by Et_3Al. This is first evidence to confirm the oxidation state of species formed after activation via their magnetic transition dipole moments.

Conclusions

In conclusion, it has been shown that the individual spectra of binary mixtures of paramagnets can be satisfactorily separated by relaxation filtered pulse EPR. These experiments require consideration of the parameter optimisation if different electronic spin states are present. Furthermore, we could identify the electronic spin states of components within model mixtures and transfer this method to a solution of activated precatalyst to obtain further evidence of Cr(III) reduction. This protocol could prove very powerful for monitoring the fate of paramagnetic catalyst precursors and intermediates during catalysis with the ultimate aim of understanding the catalytically active species and its mode of action.

Experimental

Materials

$Ph_2PN(^{i}Pr)PPh_2$ ($(^{i}Pr)PNP$)[25], **1** (**1** = $[Cr(I)(CO)_4((^{i}Pr)PNP)][Al(OC(CF_3)_3)_4]$)[26] and L-CAB (L-CAB = $[(C_{18}H_{37})_2N(CH_3)HB(C_6F_5)_4]$)[27] were synthesised following the standard procedures as reported. **2** (**2** = tris(2,2,6,6-tetramethyl-3,5-heptanedionato)chromium(III)) was obtained from Strem chemicals. $Cu(II)Cl_2$ (Sigma-Aldrich), $Mn(II)Cl_2{\cdot}4H_2O$ (Acros Organics), 2,2':6',2''-terpyridine (Alfa Aesar), NH_4PF_6 (Acros Organics) and Et_3Al (Akzo Nobel) were used as received. All solvents were obtained from Sigma-Aldrich. All manipulations for **1** and **2** complexes were carried out in a glove box (MBraun LabMaster dp) under an argon atmosphere with traces of oxygen and water below 0.1 ppm, using solvents purified and dried via standard procedures by passing through alumina and deoxygenated by freeze-pump-thaw cycles.

Synthesis of $M(II)(tpy)_2(PF_6)_2$: $Cu(II)Cl_2$ (10.3 mg, 0.06 mmol) or $Mn(II)Cl_2{\cdot}4H_2O$ (10.9 mg, 0.07 mmol) was dissolved in 16 mL of methanol and added to a solution of tpy (tpy=2,2':6',2''-terpyridine) (25.8 mg, 0.11 mmol) dissolved in 2 mL dichloromethane. The mixture was stirred at room temperature for 90 minutes and then heated to 65 °C for 1 hour. The solution was kept at room temperature and the complex was precipitated by addition of an approximate tenfold excess of NH_4PF_6 (48 mg, 0.29 mmol) powder and isolated by filtration. The solids were washed three times with cold methanol and dried in vacuo to leave a white powder (24.7 mg, 54%) for $Cu(II)(tpy)_2(PF_6)_2$ or a yellow powder for $Mn(II)(tpy)_2(PF_6)_2$ (25.7 mg, 58%) respectively. Mass spectra of these complexes showed the mass m/z 264.5 $[Cu(tpy)_2]^{2+}$ and 260.6 $[Mn(tpy)_2]^{2+}$ confirming the formation of bis-ligated complex for both Cu(II) and Mn(II), respectively.

EPR sample preparation

Model systems: 4 mM stock solutions of **1** (9.3 mg, 6 μmol) and **2** (7.2 mg, 12 μmol) were prepared in a 1:1 mixture by volume of 2-chlorotoluene (2-Cl-tol) and decahydronaphthalene (decalin). To maintain equal concentration of complexes samples of pure solutions of **1** and **2** were prepared by transferring 50 μL of stock solutions and 50 μL of solvent mixture into 4 mm quartz EPR tubes (Wilmad). The mixture containing both **1** and **2** was prepared by transferring 50 μL of each stock solution into another EPR tube. The sample tubes were sealed using rubber septa (precision seal, Sigma-Aldrich) and stored in liquid nitrogen. 1 mM solutions of **3** (**3** = $Cu(tpy)_2(PF_6)_2$, 1.2 mg, 1.5 μmol) and **4** (**4** = $Mn(tpy)_2(PF_6)_2$, 1.2 mg, 1.5 μmol) were prepared in a solvent mixture containing dimethyl sulfoxide (DMSO), ethylene glycol (EG) and deuterated water (D_2O) in the ratio 8:1:1 by volume. 35 μL of the respective solution was transferred into a 3 mm EPR tube and diluted to 70 μL with solvent mixture to prepare samples of pure compounds, whereas their mixture was prepared by mixing equal amounts of the solutions of **3** and **4** in another 3 mm EPR tube.

Precatalyst and its activation: Stock solutions of 8 mM **2** (24 mg, 40 μmol), 1 equivalent (^{i}Pr)PNP (17 mg, 40 μmol), 1.2 equivalents L-CAB (0.745 ml, 48 μmol) and 0.4 M Et_3Al (1.1 ml, 8 mmol) were prepared separately in 4-chlorotoluene (4-Cl-tol). 0.4 M stock of Et_3Al was diluted further by a factor of 5 to obtain a 0.08 M solution. Et_3Al solutions must be handled under an inert atmosphere and for *in situ* activation the Et_3Al solution was kept below the pyrophoric limit (< 0.7 M) for safe handling. The precatalyst was formed by transferring 25 μL each of the solutions of **2**, (^{i}Pr)PNP and L-CAB to a 4 mm EPR tube. The sample tube was sealed using a rubber septum. Precatalyst activation was performed outside of the glove box by injecting 25 μL of the 0.08 M Et_3Al solution (10 equivalent, 2 μmol) at room temperature, using a Hamilton® syringe flushed with argon gas. The resulting activated sample is stored in liquid nitrogen. A further control sample was prepared by adding 25

Table 1 Parameters of the inversion recovery experiment

	X-band measurements		Q-band measurements			
	Mixture of **1** and **2**		**3** (at 1167.4 mT)	**4** (at 1220 mT)	Mixture of **3** and **4**	
	at 330 mT	at 204.5 mT			at 1167.4 mT	at 1220 mT
Second frequency attenuation (dB)	0	0	0	12	0	12
Inversion pulse (ns)	16	22	16	10	20	12
τ (ns)	200	200	380	380	380	380
T (ns)	300	300	1000	1000	1000	1000
Increment in T (ns)	6000	400	20000	3000	25000	4000
srt (ms)	6	0.4	20	3	25	4

μL 4-Cl-tol instead of Et_3Al solution to the precatalyst thereby keeping the same Cr(III) concentration in both tubes.

EPR spectroscopy

All measurements on **1** and **2** were performed using X-band frequencies (~9.7 GHz) using a Bruker Elexsys E580 EPR spectrometer with a flex line probe head and an MD5 dielectric ring resonator. All experiments on **3** and **4** were done at Q-band frequencies (~34 GHz) using a QT-II resonator. Pulses were amplified by travelling wave tube (TWT) amplifiers (1 kW at X-band and 150 W at Q-band) from Applied Systems Engineering. The sample temperature was stabilized to 10 K with a variable temperature helium flow cryostat (Oxford Instruments) at X-band and with a cryogen-free variable temperature cryostat from Cryogenic Ltd at Q-band.

Echo detected field sweep experiments ($\pi/2-\tau-\pi-\tau$) were optimised for maximum echo amplitude. The pulse lengths were set to 32 ns for the π pulse and 16 ns for the π/2 pulse. Shot repetition times (srt – the inverse experiment repetition rate) of 6 ms for **3**, 1 ms for **4**, 2 ms for **1** and 0.2 ms for **2** were used. Echo detected field sweep experiments were recorded at microwave power levels of 2 dB for **1**, 7 dB for **2**, 5 dB for **3** and 17 dB for **4** (note the different microwave frequencies and power levels as above). The parameters used for inversion recovery experiments ($\pi-T-\pi/2-\tau-\pi-\tau$) are given in Table 1. In addition, a 2-step phase cycle [(x) − (–x)] was applied to cancel any receiver offset. A relaxation filter experiment was performed using an inversion recovery sequence with a constant time T, where the longitudinal magnetisation of one species has a zero crossing when recovering from inversion. In addition, echo detected transient nutation was performed on the different species. Hereto a pulse with variable length *t* instead of π ($t-T-\pi/2-\tau-\pi-\tau$) is used to record the transient nutation of the electron spins and estimate the spin state. For the precatalyst, microwave power of 5 dB, srt of 0.2 ms were used in contrast with microwave power of 5 dB, srt of 2 ms for the species obtained after activation.

Conflicts of interest

There are no conflicts to declare.

Acknowledgements

This work was supported by Sasol Ltd. SC is grateful for a St Leonard's postgraduate fellowship by the University of St Andrews. We are indebted to Prof. David Cole-Hamilton for insightful discussions. We thank Clemence Devalliere for the preparation of terpyridine complexes of Cu(II) and Mn(II) and Prof. Snorri Sigurdsson for providing a triarylmethyl radical as a generous gift. We further thank the EPSRC UK National Mass Spectrometry Facility at Swansea University.

References

1. P. Chirik and R. Morris, *Acc. Chem. Res.*, 2015, **48**, 2495-2495.
2. J. F. Jenck, F. Agterberg and M. J. Droescher, *Green Chem.*, 2004, **6**, 544-556.
3. J. M. Brown, *J. Organomet. Chem.*, 2004, **689**, 4006-4015.
4. P. S. Pregosin, *NMR in Organometallic Chemistry*, Wiley-VCH, Weinheim, 2012.
5. S. Van Doorslaer and D. Murphy, in *EPR Spectroscopy*, eds. M. Drescher and G. Jeschke, Springer, Berlin, Heidelberg, 2012, 1, 1-39.
6. M. Goswami, A. Chirila, C. Rebreyend and B. de Bruin, *Top. Catal.*, 2015, **58**, 719-750.
7. K. A. Alferov, G. P. Belov and Y. Meng, *Appl. Catal., A*, 2017, **542**, 71-124.
8. D. S. McGuinness, *Chem. Rev.*, 2010, **111**, 2321-2341.
9. J. Rabeah, M. Bauer, W. Baumann, A. E. C. McConnell, W. F. Gabrielli, P. B. Webb, D. Selent and A. Brückner, *ACS Catal.*, 2013, **3**, 95-102.
10. A. Bollmann, K. Blann, J. T. Dixon, F. M. Hess, E. Killian, H. Maumela, D. S. McGuinness, D. H. Morgan, A. Neveling, S. Otto, M. Overett, A. M. Z. Slawin, P. Wasserscheid and S. Kuhlmann, *J. Am. Chem. Soc.*, 2004, **126**, 14712-14713.
11. A. Brückner, J. K. Jabor, A. E. C. McConnell and P. B. Webb, *Organometallics*, 2008, **27**, 3849-3856.
12. A. J. Rucklidge, D. S. McGuinness, R. P. Tooze, A. M. Z. Slawin, J. D. A. Pelletier, M. J. Hanton and P. B. Webb, *Organometallics*, 2007, **26**, 2782-2787.
13. E. Carter, K. J. Cavell, W. F. Gabrielli, M. J. Hanton, A. J. Hallett, L. McDyre, J. A. Platts, D. M. Smith and D. M. Murphy, *Organometallics*, 2013, **32**, 1924-1931.
14. G. R. Eaton and S. S. Eaton, *J. Magn. Reson.*, 1987, **71**, 271-275.
15. T. Maly, F. MacMillan, K. Zwicker, N. Kashani-Poor, U. Brandt and T. F. Prisner, *Biochemistry*, 2004, **43**, 3969-3978.

16. A. Schweiger and G. Jeschke, *Principles of pulse electron paramagnetic resonance*, Oxford University Press, New York, 2001.
17. A. V. Astashkin and A. Schweiger, *Chem. Phys. Lett.*, 1990, **174**, 595-602.
18. V. Kouskov, D. J. Sloop, S.-B. Liu and T.-S. Lin, *J. Magn. Reson., Ser. A*, 1995, **117**, 9-15.
19. S. Stoll, G. Jeschke, M. Willer and A. Schweiger, *J. Magn. Reson.*, 1998, **130**, 86-96.
20. H. Bock, K. Gharagozloo-Hubmann, M. Sievert, T. Prisner and Z. Havlas, *Nature*, 2000, **404**, 267.
21. M. I. Arriortua, T. Rojo, J. M. Amigo, G. Germain and J. P. Declercq, *Acta Crystallogr., Sect. B*, 1982, **38**, 1323-1324.
22. A. Meyer, G. Schnakenburg, R. Glaum and O. Schiemann, *Inorg. Chem.*, 2015, **54**, 8456-8464.
23. C. Duboc, *Chem. Soc. Rev.*, 2016, **45**, 5834-5847.
24. A. Cernescu, T. Maly and T. F. Prisner, *J. Magn. Reson.*, 2008, **192**, 78-84.
25. K. Blann, A. Bollmann, H. de Bod, J. T. Dixon, E. Killian, P. Nongodlwana, M. C. Maumela, H. Maumela, A. E. McConnell, D. H. Morgan, M. J. Overett, M. Prétorius, S. Kuhlmann and P. Wasserscheid, *J. Catal.*, 2007, **249**, 244-249.
26. D. S. McGuinness, D. B. Brown, R. P. Tooze, F. M. Hess, J. T. Dixon and A. M. Z. Slawin, *Organometallics*, 2006, **25**, 3605-3610.
27. R. K. Rosen and D. D. VanderLende, US Pat., 5919983A, 1999.